Dynamic analysis of the interaction between unconfined turbidity currents and obstacles

Richard I. Wilson and Heide Friedrich
The University of Auckland, New Zealand

Sediment underflows, commonly known as turbidity currents, are a type of gravity current that occurs in deep oceans, lakes and river mouths. The present work studies the interaction of turbidity currents with different obstacles and substrates using the ultrasonic Doppler velocity profiler (UDVP) measurement technique in an unconfined basin with a lockbox. The following four conditions are tested: (a) flow of a turbidity current over a smooth surface, (b) flow over a smooth surface with an obstacle present, (c) flow over a rough surface and (d) flow over a rough surface with an obstacle present. It is observed that a rough surface significantly reduces current velocities and diminishes the presence of Kelvin-Helmholtz billows. The presence of a square-cylinder obstacle causes local regions of increased and decreased velocity, but does not have an effect on the global current velocity. Turbulence intensities are slightly higher than presented in previous confined studies.

Keywords: Turbidity current, ultrasonic Doppler velocity profiler, basin, obstacle, substrate

1 INTRODUCTION

Sedimentary environments such as lakes, seas and deep oceanic shelves commonly contain clay-rich, submarine underflows, which behave in a manner much differently to generic clear-water turbulent flows [1]. These clay-rich underflows, predominantly referred to as turbidity currents, are the major contributors to sediment transport in lakes and oceans [2]. If large enough, these currents mobilise a substantial amount of sediment, causing an ignitive continuum of turbid current flow [3].

Turbidity currents are important to engineers as they pose many potential environmental hazards such as sub-marine cable-breakage and reservoir sedimentation [4]. They are also one of the main catalysts of geological sea-bed formation and stratigraphy, including many of the earth's largest oil reservoirs [5]. Complex numerical solutions of the mechanics behind turbidity currents are much sought after, as they enable engineers to artificially model turbidite formation in order to predict long term events [4]. Laboratory experiments focusing on the velocity profiles of small-scale turbidity currents is at present the most popular method of model research [6].

The following paper presents a study on the interaction of turbidity currents with different obstacle and bed substrate configurations. Unconfined turbidity currents are analyzed, using UDVP (ultrasonic Doppler velocity profiler) instrumentation for four different testing configurations: (A) A smooth bed surface with no obstacle; (B) A smooth bed surface with a square-bottomed cylinder running perpendicular to flow direction, located on the basin bed; (C) A rough, sand-like surface with no obstacle; (D) A rough, sand-like surface current with a square-bottomed cylinder running perpendicular to flow direction.

2 METHODOLOGY

2.1 Experimental Setup

Testing was conducted in an unconfined, rectangular basin at the University of Auckland. The basin was a hybrid construction of plywood and Perspex glass, situated on a concrete floor. It had a length of 2420 mm, width of 2000 mm and sides with a height of 600 mm. More testing environment information and background of the sediment concentrations used to model the turbidity current is presented in [7].

For the testing of currents over a rough substrate (setups C and D), a 4 mm layer of silicon plastic with 0.8 mm diameter sand glued on the top was installed above the glass floor to create a rough surface. For the testing conditions involving an obstacle (setups B and D), a 20 mm x 20 mm aluminium cylinder was located along the width of the basin at a distance of 1481.25 mm from the lockbox end. The testing of the current over a smooth substrate with no obstacle (setup A), was conducted solely involving the false glass floor.

2.2 Velocity Measurement

[8] used 6 horizontal transducers whilst [9] used 10 horizontal transducers to analyse turbidity currents. [10] however used 5 horizontal and 5 vertical transducers. For this study it was chosen to allocate nine horizontal transducers and 5 vertical transducers in order to focus on gaining horizontal profiles, yet also obtain certain vertical profiles. A custom Perspex rig was designed to hold UDVP transducers, positioned at a location in the centerline of the basin, where they had least influence on flow. Figure 1 shows the configuration of all 14 transducers.

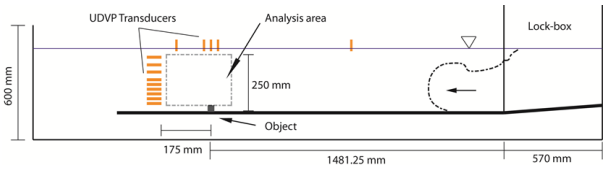

Figure 1: Side-view of the unconfined basin, including the analysis area and positioning of the square-cylinder obstacle. The transducers are labeled 1-14, going clockwise from the lowest horizontal transducer.

The horizontal transducer positioning was based off [9], although an initial test provided information of the current head height within the setup, allowing alignment of the horizontal transducers at an appropriate range. All transducers, except for 14, were positioned to record horizontal and vertical velocity profiles inside a nominated 'analysis area' (Figure 1). Thus, the dynamics of the flow immediately before and after the obstacle location could be analysed. Transducer 14 was located near the lockbox to be a reference if needed, however it was not used in the analysis.

UDVP settings were based off those used by [10], and optimised to the conditions of the basin. It was chosen to use 128 virtual channels, evenly spaced out over a measurement range of 26-238 mm from the transducer tip. A number of test runs were conducted to make sure there was no unwanted signal noise for any of the channels. This was governed by maintaining a low SNR (signal-to-noise) ratio. When measuring, the transducers continuously cycled through from 1-14. This caused a trade-off between data quality and time resolution. If a higher data quality was desired, the number of signal repetitions could be increased. Two different UDVP settings were used in the official testing of the obstacle configurations A, B, C and D. The first had 16 signal repetitions with a full transducer cycle time of 1.27s. The second setting had 32 repetitions, giving a full cycle time of 1.45s. In the end it was chosen to use the latter setting because of data quality.

2.3 Data Processing

Processing of the UDVP data was undertaken in MATLAB. The raw velocity data was first filtered for unwanted spikes and noise. A method similar to [11] was implemented. All the velocity profiles recorded for each transducer were separated. The velocity of each individual channel, per transducer, was then ordered chronologically (e.g. Channel 1 of transducer 1, for all recorded cycles). A standard deviation of each channel was then calculated (time-wise). This was achieved by using a moving average window of 10 velocity readings for each channel over time, as the nature of the turbidity current was not continuous. All velocity readings which were outlying two standard deviations were replaced with a three-point moving mean. This deviation width was chosen because it was used by [11], and removed the most spikes compared to other deviation widths, whilst not excessively removing data. The data was not altered by more than 6%, which was considered acceptable. Because the transducers could not record simultaneously, a method of time interpolation similar to [10] was implemented. The velocities of each transducer were interpolated with time, using piecewise cubic Hermite interpolation. The time interpolation approximated an instantaneous velocity recording of all transducers for each full cycle, at a time which was equal to the average time in each cycles' time range.

3 RESULTS

Figure 2 shows horizontal velocity contour plots of the analysis area. The blue regions represent a negative (forward) velocity whilst the yellow regions represent a positive (backwards) velocity. Directional flow vectors were generated at the intersecting points of the horizontal and vertical transducer beams. Figure 2a shows the first cycle, when the turbidity current reached the analysis area. The displayed cycle number above each plot refers to the cycle number relative to when the UDVP machine initiated data recording for each obstacle setup. The slight differences in these cycle times are due to human inaccuracy of opening the lockbox with consistent timing. The initial turbidity current surge was visually identified for each setup. Figure 2b shows the third cycle, whilst Figure 2c displays the tenth and final cycle which was included in the analysis. Cycles 2 and 4-9 were also used in the analysis. However, cycles 1, 3 and 10 provided the best representation of features seen in the current behaviour. Average velocities were calculated using a moving time window of 3 cycles and turbulence intensities were calculated for 10 cycles after the current had reached the analysis area. Turbulence intensity was pointed out by [12] as a popular means of calculating the turbulence of turbidity currents. It was implemented by [12], [9] and [8]. Because of extra noise encountered with the vertical transducers in setups C and D (from the rough bed surface), it was decided not to plot turbulence intensities in the same manner as [12], who calculated their intensities from a vertically placed transducer. Therefore the horizontal transducers' relative position in the basin was plotted vertically against intensity. The channels of the transducers were divided into five spatial regions (Figure 3a). The calculated intensities for each transducer were then averaged for each region (Figure 3b). The regions were based off research by [13].

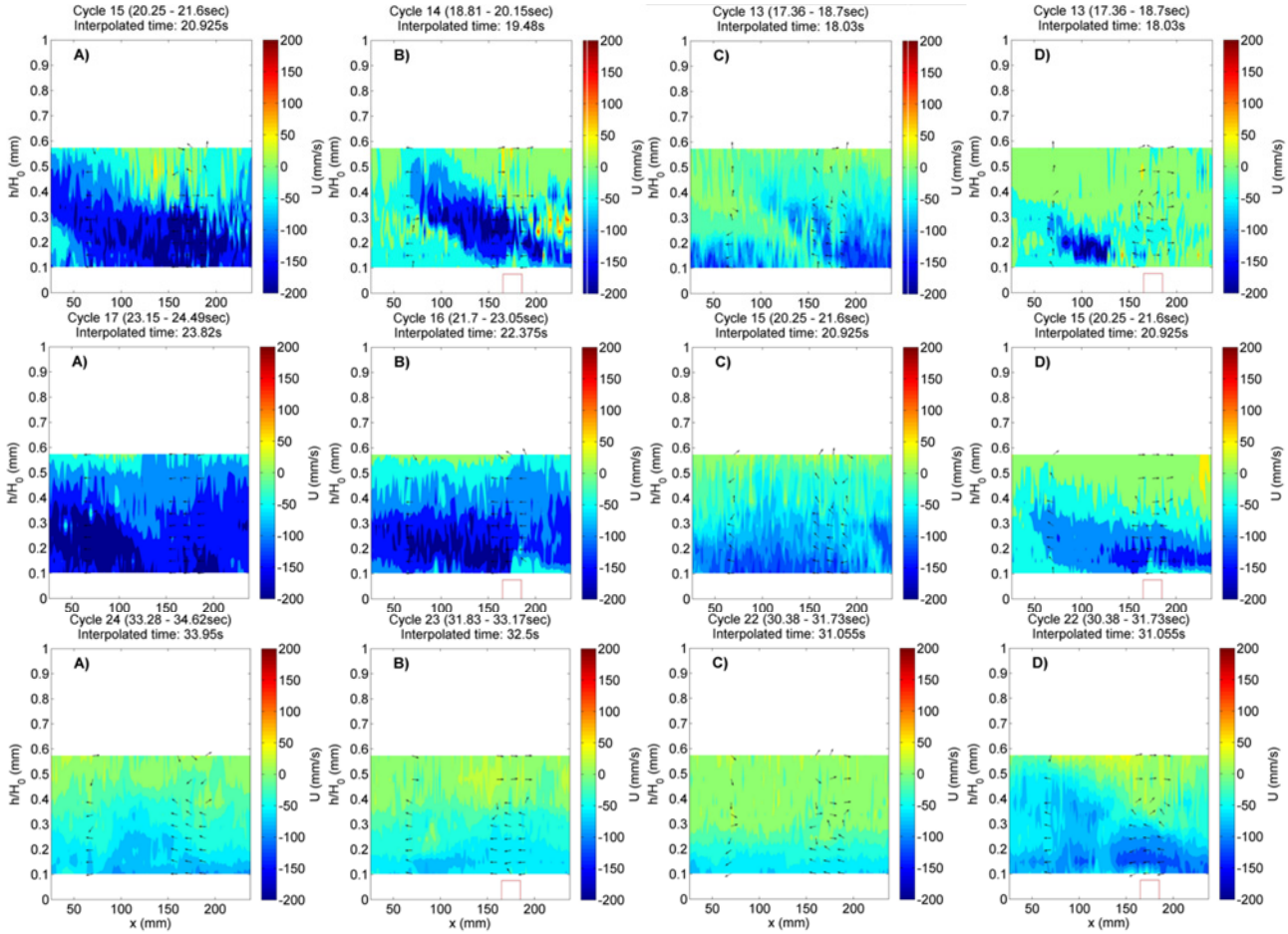

Figure 2: Horizontal velocity contour plots with directional vectors of setup A, B, C and D; (top) first cycle; (middle) third cycle; (bottom) tenth cycle. The x-axis represents distance from horizontal transducer tips.

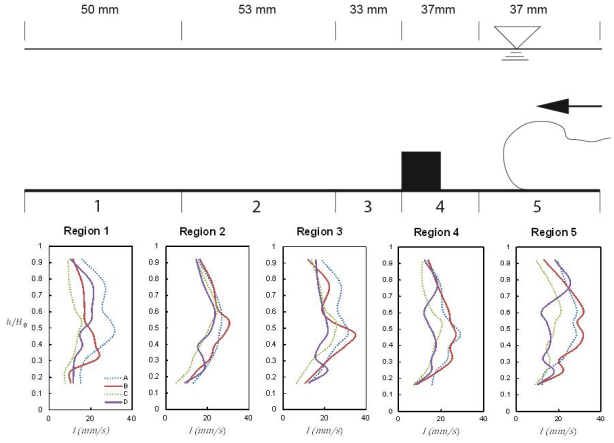

Figure 3: (a) Side-view of the five regions of intensity analysis; (b) Vertical turbulence intensities profiles.

Table 1: Intensity statistics for all regions.

	Turbulence Intensity (mm/s)			
Setup	A	B	C	D
I_{mean}	22.1	20.6	14.8	16.2
I_{max}	31.5	34.7	25.4	25.4
I_{min}	12.3	8.4	5.0	7.8
I_{range}	19.1	26.3	20.4	17.6

For this study, the regions were slightly different to [13], as they were adjusted to trends which were evident when looking at non-averaged intensity plots of each individual transducer. The average intensity for each setup (A, B, C and D) over all the regions was calculated (Table 1).

4 DISCUSSION

All four configurations showed a similar shape in the current head first cycle, when the current reached the analysis area (Figure 2a). A long overhanging current, more prevalent in setups A and B, could be seen. The head in B appears to detach itself from the base more than A, after reaching the obstacle. However, more testing is needed to determine whether this is a recurring trend. Setup A had the largest surge, with the majority of the current having horizontal velocities over 100 mm/s. Both setups A and B showed regions of positive (backwards) velocity behind the current head. This suggests the presence of Kelvin-Helmholtz billows. Setups C and D are void of such velocities, showing that the rough surface diminishes the effect of billows. C and D also have less intense velocities than A and B, showing that the rough surface also slows down the turbidity current. Both B and D showed a region of increased velocity directly after the obstacle, suggesting the obstacle causes intensified local eddies to be formed. A region of decreased velocity before and above the surface of the obstacle was also present for both B and D,

showing the obstacle induces local resistance to flow. Figure 2b shows the currents have reached a more composed state. Setup A continues to have the largest velocities of all different obstacle configurations. Setup B has slightly less intense velocities, with the local regions of increased and decreased velocities (Figure 2a) still present. Setup D, which has significantly less intense velocities than B, continues to show these local regions of increased/decreased velocities. Setup C has much less intense velocities than its smooth surface equivalent, A. Figure 2c shows the velocities of the remaining current for all transducers significantly diminished. All setups showed a relatively consistent vertical gradient of velocities, with slight forward flow near the bed, and stationary or slightly backwards flow at the normalised height of 0.6. Interestingly, forward velocities of setup D appeared to slightly increase in magnitude during the last cycles. This may have been caused by the combination of the obstacle with a rough surface, or from how the lockbox was manually opened. The intensities calculated for all four setups averaged between 15-22 mm/s. Setup A had an average intensity of 22.1 mm/s (see Table 1). This is slightly higher than [12]'s calculated intensities of a confined turbidity current over a smooth surface. This suggests that turbidity currents may have a greater turbulence in unconfined conditions. However, [12] calculated their intensities from vertical velocity readings, whereas this study used horizontal velocities. This may explain a significant difference between this study and [12]'s results. They found an area of maximum intensity to be present above the flume bed, whereas the results in this study (Figure 3b) showed intensities to decrease towards the basin bed. However, [12] found this area of maximum intensity to be between heights of 5-10 mm which is outside the measured area in this study. The regional intensity plots (Figure 3b) clearly show that setups A and B consistently had higher velocities than setups C and D. This shows that the rough substrate significantly reduces the global velocity of the turbidity current, but the obstacle only causes local fluctuations of velocity.

5 CONCLUSIONS

New insights into the nature of unconfined turbidity currents and their interactions with obstacles and substrates are presented. The rough substrate was found to have significantly slowed down the turbidity current propagation and visual observations showed a reduction of Kelvin-Helmholtz billows behind the current heads. The presence of an obstacle did not have much effect on the global velocity of currents, however, in the region before the obstacle, minimal velocities were observed, indicating flow resistance. Conversely, the region after the obstacle showed increased velocities. This suggested eddies to be present, which in a natural setting may cause undermining of submarine structures. The calculated intensities were of a slightly higher range then that of [12], and did not show an area of increased intensity near the basin bed. This was likely due to the intensities being recorded in a different spatial dimension, and readings not being taken as close to the bed. The results of this study clearly show that future research should implement a rough bed surface, if testing is to be representative of natural currents.

REFERENCES

[1] Baas J H & Best J L: Turbulence modulation in clay-rich sediment-laden flows and some implications for sediment deposition, Journal of Sedimentary Research, 72 (2002), 336-340.

[2] Kneller B & Buckee C: The structure and fluid mechanics of turbidity currents: a review of some recent studies and their geological implications, Sedimentology, 47 (2000), 62-94.

[3] Meiburg E & Kneller B: Turbidity currents and their deposits, Ann. Rev. of Fluid Mec., 42 (2010), 135-156.

[4] Middleton G V: Sediment deposition from turbidity currents, Annual Review of Earth and Planetary Sciences, 21 (1993), 89-114

[5] Weimer P & Link M H: Global petroleum occurrences in submarine fans and turbidite systems, AAPG Bulletin, 74 (1990), 9-67.

[6] Felix M, et al.: Combined measurements of velocity and concentration in experimental turbidity currents, Sedimentary Geology, 179 (2005), 31-47.

[7] McArthur JM, et al.: Photometric analysis of the effect of substrates and obstacles on unconfined turbidity current flow propagation, Proc River Flow 2014.

[8] Choux, et al.: Comparison of spatio-temporal evolution of experimental particulate gravity flows at two different initial concentrations, based on velocity, grain size and density data, Sed. Geo., 179 (2005), 49-69.

[9] Gray T E, et al.: Longitudinal flow evolution and turbulence structure of dynamically similar, sustained, saline density and turbidity currents, J. Geophys. Res., 111 (2006), C08015.

[10] Gray T E, et al.: Quantifying velocity and turbulence structure in depositing sustained turbidity currents across breaks in slope, Sedim., 52 (2005), 467-488.

[11] Keevil G M, et al.: Flow structure in sinuous submarine channels: Velocity and turbulence structure of an experimental submarine channel, Marine Geology, 229 (2006), 241-257.

[12] Eggenhuisen J T & Mccaffrey W D: The vertical turbulence structure of experimental turbidity currents encountering basal obstructions: implications for vertical suspended sediment distribution in non-equilibrium currents, Sedim., 59 (2012), 1101-1120.

[13] Gonzalez-Juez E, et al.: Gravity currents impinging on bottom-mounted square cylinders: flow fields and associated forces, J. of Fld. Mec., 631 (2009b), 65-102.